

An overlapping splitting double sweep method for the Helmholtz equation

Nacime Bouziani*, Henri Calandra[†], Frédéric Nataf[‡]

Contents

1	Introduction	1
2	Statement of the problem and some algorithms	2
3	Overlapping Splitting double sweep	3
3.1	Substructuring	3
3.2	Overlapping Splitting Double Sweep preconditioner (OSDS)	4
4	Convergence rates	5
4.1	Application to Helmholtz equation	7
4.1.1	Propagative modes $ \xi < k $	7
4.1.2	Vanishing modes $ \xi > k $	8
5	Numerical results	8
5.1	Homogeneous waveguide	9
5.2	Influence of the overlap	9
5.3	Open cavity test	11
5.4	Wedge test	11
6	Prospects	13

Abstract

We consider the domain decomposition method approach to solve the Helmholtz equation. Double sweep based approaches for overlapping decompositions are presented. In particular, we introduce an overlapping splitting double sweep (OSDS) method valid for any type of interface boundary conditions. Despite the fact that first order interface boundary conditions are used, the OSDS method demonstrates good stability properties with respect to the number of subdomains and the frequency even for heterogeneous media. In this context, convergence is improved when compared to the double sweep methods in [13] and [16, 17] for all of our test cases: waveguide, open cavity and wedge problems.

1 Introduction

Solving the Helmholtz equation numerically is a difficult task, especially when dealing with high-frequency regimes, heterogeneous media or reflecting boundary conditions. Over the last decades a lot of effort and progress has been made in developing efficient algorithms to solve the ill-conditioned linear system resulting from the Helmholtz operator's discretization. Domain decomposition methods (DDM) try to overcome these difficulties. They are hybrid methods that combine direct solvers in subdomains and iterative matching of the solutions across the subdomains. The original domain decomposition method introduced by Schwarz [15] only works for overlapping domain decomposition. P. L. Lions [12] introduced a new variant of this algorithm where the Dirichlet interface conditions are replaced by Robin interface conditions, his method can be applied to both overlapping and nonoverlapping subdomains. He showed convergence for the elliptic case and the proof was extended by Després [4] to the Helmholtz equation and later on to the time-harmonic Maxwell equations [5]. It is known

*Department of Mathematics, Imperial College London, London, SW7 2AZ, UK (n.bouziani18@imperial.ac.uk)

[†] TOTAL, Centre Scientifique et Technique Jean F  ger, avenue de Larribau F-64000 Pau, France (henri.calandra@total.com)

[‡] Laboratoire J.L. Lions, Universit   Pierre et Marie Curie, 4 place Jussieu, 75005 Paris, France, and ALPINES INRIA, Paris, France (frederic.nataf@sorbonne-universite.fr)

that the presence of overlaps helps to speed up the convergence, however nonoverlapping based methods are often used to avoid to deal with the construction of the normal derivative of the solution. More recently, sweeping-type domain decomposition methods have been made popular due to their capability to achieve nearly-linear asymptotic complexity. A sweeping algorithm was first proposed and analyzed in [13] for convection-diffusion operators. Sweeping approaches for Helmholtz problems have recently seen its interest renewed as a preconditionner to speed up the convergence of the solver: the double sweep preconditionner of Vion and Geuzaine for non overlapping decomposition with high order interface conditions [16, 17], the PML-based sweep method of Stolk [2], and the polarized traces method of Zepeda-Núñez and Demanet [18]. There also exists sweeping-type methods that are not domain decomposition based methods, such as the sweeping PML preconditionner of Engquist and Ying [8, 7], the source transfer method [3], see [10] for a complete panorama and relations between these methods.

For a decomposition of the domain into layers and when equipping the local subproblems with exact absorbing boundary conditions (ABC), the total number of iterations is equal to the number of subdomains, this is due to the nilpotency of the iteration operator valued matrix. In practice, the exact ABC (which are also the optimal interface conditions, see [14]) procedure is tedious to implement and computationally expensive. On the other hand, for the non-exact ABC such as Robin condition, the nilpotency property is lost and convergence deteriorates. More precisely, these boundary conditions at the interfaces produce spurious reflected waves that significantly increase the number of iterations to converge, in particular for heterogeneous media and high frequency regimes.

We propose to precondition the discrete Helmholtz system by an overlapping splitting double-sweep algorithm that allows for overlapping subdomains and prevents spurious interface reflections from hindering the convergence. Enabling overlapping subdomains enables to leverage its beneficial effect on the damping of high frequency modes (see e.g. [6], § 2.2.) of the error whereas the splitting prevents its adversary effect on the convergence of propagative modes. This is useful since in the non-overlapping approach [16, 17], the quality of the ABC is nearly the only way of impacting the convergence of the algorithm, and when dealing with more complex problem such as Maxwell equations high order ABCs are harder to handle.

Note that in double sweep algorithms only one or two subdomain solves are done concurrently. In order to avoid having idle processes, in [17] it is proposed to pipeline the algorithm with respect to multiple right hand sides. This is useful in seismic inversion problems or in far-field pattern computations.

We will first state the problem in § 2. Then we explain in § 3 how we substructure the Helmholtz problem and formulate a modified version of the double sweep algorithms introduced in [13, 16, 17], then how we use this overlapping splitting double sweep algorithm to build a preconditionner that efficiently speed up the convergence of the solver. In § 4, the convergence of the algorithm is studied when it is applied to a decomposition of the plane into vertical strips. In § 5, we present numerical results for the original problem, i.e. the Helmholtz problem.

2 Statement of the problem and some algorithms

We consider the Helmholtz equation in a bounded domain $\Omega \subset \mathbb{R}^2$ with frequency ω , velocity c and wavenumber k defined by $k^2 = \omega^2/c^2$:

$$\begin{aligned} (-k^2 - \Delta) u &= f \text{ in } \Omega \\ &+ \text{appropriate boundary conditions on } \partial\Omega. \end{aligned} \quad (1)$$

We consider a layered decomposition of Ω into N slices $(\Omega_i)_{1 \leq i \leq N}$ without overlap, see Figure 1. More precisely, for each $1 \leq i \leq N$, $\Omega \setminus \Omega_i$ is written as the disjoint union of two open subsets $\Omega_{i,l}$ and $\Omega_{i,r}$ where $\Omega_{i,l}$ is on the left of Ω_i and $\Omega_{i,r}$ on its right. The boundary $\partial\Omega_i \setminus \partial\Omega$ is written as the disjoint union of $\Gamma_{i,l}$ and $\Gamma_{i,r}$ where $\Gamma_{i,l}$ is on the left of Ω_i and $\Gamma_{i,r}$ is on its right ($\Omega_{1,l} = \emptyset$ and $\Omega_{N,r} = \emptyset$) (see Fig. 2). The outward normal from Ω_i on $\Gamma_{i,l}$ (resp. $\Gamma_{i,r}$) is denoted by $\vec{n}_{i,l}$ (resp. $\vec{n}_{i,r}$). The problem (1) can be solved iteratively using a domain decomposition method where we solve locally on each subdomain

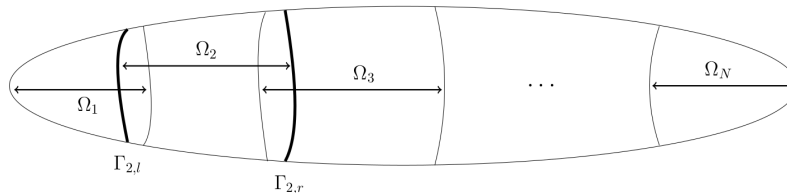


Figure 1: Decomposition into vertical strips

Ω_i the equation (1) with appropriate boundary conditions on the physical boundaries and interfaces [4]. The method writes: Solve in parallel:

$$\begin{cases} (-k^2 - \Delta) u_i^{n+1} = f & \text{in } \Omega_i, \ 1 \leq i \leq N \\ \mathcal{B}_{i,l}(u_i^{n+1}) = \mathcal{B}_{i,l}(u_{i-1}^n) & \text{on } \Gamma_{i,l}, \ 2 \leq i \leq N \\ \mathcal{B}_{i,r}(u_i^{n+1}) = \mathcal{B}_{i,r}(u_{i+1}^n) & \text{on } \Gamma_{i,r}, \ 1 \leq i \leq N-1 \\ \text{+ appropriate boundary conditions on } \partial\Omega \cap \partial\Omega_i. \end{cases} \quad (2)$$

where $\mathcal{B}_{i,l}$ and $\mathcal{B}_{i,r}$ are the interface conditions. For sake of simplicity, we consider first-order ABC as interface conditions:

$$\begin{cases} \mathcal{B}_{i,l} = \partial_{\vec{n}_{i,l}} + Ik \\ \mathcal{B}_{i,r} = \partial_{\vec{n}_{i,r}} + Ik \end{cases} \quad (3)$$

where $I^2 = -1$ and $\vec{n}_{i,r}$ (resp. $\vec{n}_{i,l}$) is the outward normal to domain Ω_i on $\Gamma_{i,r}$ (resp. $\Gamma_{i,l}$). It is known that higher-order ABC lead to significative improve of the convergence speed, see e.g. [9, 1].

A more efficient variant of algorithm 2 was introduced in [13]. It consists in double sweeps over the subdomains:

Left to right sweep:

$$\begin{cases} (-k^2 - \Delta) u_i^{n+1/2} = f & \text{in } \Omega_i, \ 1 \leq i \leq N \\ \mathcal{B}_{i,l}(u_i^{n+1/2}) = \mathcal{B}_{i,l}(u_{i-1}^{n+1/2}) & \text{on } \Gamma_{i,l}, \ 2 \leq i \leq N \\ \mathcal{B}_{i,r}(u_i^{n+1/2}) = \mathcal{B}_{i,r}(u_{i+1}^n) & \text{on } \Gamma_{i,r}, \ 1 \leq i \leq N-1 \\ \text{+ appropriate boundary conditions on } \partial\Omega \cap \partial\Omega_i. \end{cases} \quad (4)$$

Right to left sweep:

$$\begin{cases} (-k^2 - \Delta) u_i^{n+1} = f & \text{in } \Omega_i, \ 1 \leq i \leq N \\ \mathcal{B}_{i,l}(u_i^{n+1}) = \mathcal{B}_{i,l}(u_{i-1}^{n+1/2}) & \text{on } \Gamma_{i,l}, \ 2 \leq i \leq N \\ \mathcal{B}_{i,r}(u_i^{n+1}) = \mathcal{B}_{i,r}(u_{i+1}^{n+1}) & \text{on } \Gamma_{i,r}, \ 1 \leq i \leq N-1 \\ \text{+ appropriate boundary conditions on } \partial\Omega \cap \partial\Omega_i. \end{cases} \quad (5)$$

3 Overlapping Splitting double sweep

In this section, we define a variant of algorithm (4)-(5) which has a superior convergence. Numerical results will show that it benefits better from the overlap and have a better parallelism. This algorithm is written in terms of the substructured problem that we define first.

3.1 Substructuring

Substructuring the algorithm (2), the iterative method can be reformulated considering only surfacic unknowns on the interfaces:

$$\begin{cases} h_{i,l}^n := \mathcal{B}_{i,l}(u_i^n), & \text{on } \Gamma_{i,l} \text{ for } 2 \leq i \leq N \\ h_{i,r}^n := \mathcal{B}_{i,r}(u_i^n), & \text{on } \Gamma_{i,r} \text{ for } 1 \leq i \leq N-1. \end{cases} \quad (6)$$

Considering the global vector h^n containing the local unknowns $(h_{i,l}^n)_{2 \leq i \leq N}$ and $(h_{i,r}^n)_{1 \leq i \leq N-1}$, we can reformulate the additive Schwarz method (2) as a Jacobi algorithm on h^n :

$$h^{n+1} := \mathcal{T}(h^n) + G \quad (7)$$

where the iteration operator \mathcal{T} can be written in the form of an operator valued matrix and G refers to the contribution of the right-hand side f , see [14]. Therefore, we look for a vector h such that,

$$(Id - \mathcal{T})(h) = G. \quad (8)$$

In order to define more precisely the operator \mathcal{T} , we introduce for each subdomain an operator S_i which takes three arguments, two surfacic functions h_l and h_r and a volume function f :

$$S_i(h_l, h_r, f) := v \quad (9)$$

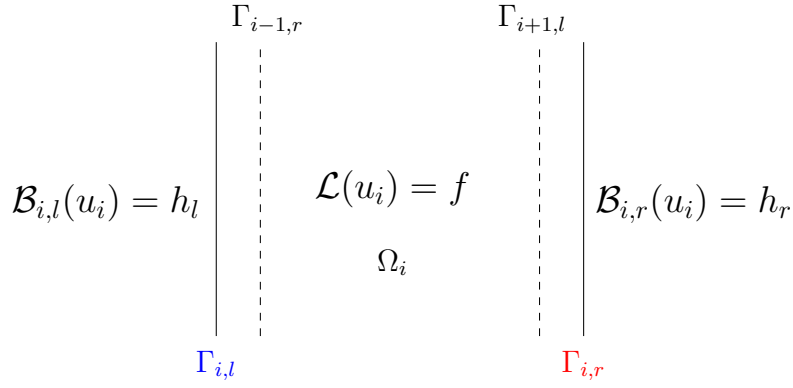


Figure 2: Local problem on the subdomain Ω_i

where $v : \Omega_i \mapsto \mathbb{C}$ satisfies:

$$\begin{cases} (-k^2 - \Delta) v = f & \text{in } \Omega_i \\ \mathcal{B}_{i,l}(v) = h_l & \text{on } \Gamma_{i,l} \quad (2 \leq i \leq N) \\ \mathcal{B}_{i,r}(v) = h_r & \text{on } \Gamma_{i,r} \quad (1 \leq i \leq N-1) \\ + \text{ appropriate boundary conditions on } \partial\Omega \cap \partial\Omega_i, \end{cases} \quad (10)$$

for $1 < i < N$. For $i = 1$, the definition of S_1 is similar except that it takes only the two arguments (h_r, f) since domain Ω_1 has no left interface and similarly operator S_N takes only the two arguments (h_l, f) since domain Ω_N has no right interface. **As of now, for sake of simplicity and by abuse of notation, $S_1(h_l, h_r, f)$ (resp. $S_N(h_l, h_r, f)$) will refer to $S_1(h_r, f)$ (resp. $S_N(h_l, f)$).**

Next, we introduce the surfacic right hand-side G by

$$\begin{aligned} G_{i+1,l} &:= \mathcal{B}_{i+1,l}(S_i(0, 0, f)), \quad 1 \leq i \leq N-1 \\ G_{i-1,r} &:= \mathcal{B}_{i-1,r}(S_i(0, 0, f)), \quad 2 \leq i \leq N. \end{aligned} \quad (11)$$

and the substructured operator \mathcal{T} by:

$$\begin{aligned} \mathcal{T}(h)_{i+1,l} &:= \mathcal{B}_{i+1,l}(S_i(h_{i,l}, h_{i,r}, 0)), \quad 1 \leq i \leq N-1 \\ \mathcal{T}(h)_{i-1,r} &:= \mathcal{B}_{i-1,r}(S_i(h_{i,l}, h_{i,r}, 0)), \quad 2 \leq i \leq N. \end{aligned} \quad (12)$$

Using this framework, we write the substructured form of the **double sweep algorithm** as follows:

Forward sweep

$$\begin{aligned} h_{i+1,l}^{n+1/2} &:= \mathcal{B}_{i+1,l}(S_i(h_{i,l}^{n+1/2}, h_{i,r}^n, f)), \\ h_{i-1,r}^{n+1/2} &:= \mathcal{B}_{i-1,r}(S_i(h_{i,l}^{n+1/2}, h_{i,r}^n, f)), \end{aligned} \quad (13)$$

followed by a Backward sweep

$$\begin{aligned} h_{i+1,l}^{n+1} &:= \mathcal{B}_{i+1,l}(S_i(h_{i,l}^{n+1/2}, h_{i,r}^{n+1}, f)), \\ h_{i-1,r}^{n+1} &:= \mathcal{B}_{i-1,r}(S_i(h_{i,l}^{n+1/2}, h_{i,r}^{n+1}, f)). \end{aligned} \quad (14)$$

3.2 Overlapping Splitting Double Sweep preconditioner (OSDS)

We explain now the rationale behind the overlapping splitting double sweep preconditioner that we define in this section. Note first that by linearity of the operators $(S_i)_{1 \leq i \leq N}$, the contribution of each subdomain can be split into two contributions, one for each of its two interfaces:

$$\begin{aligned} \mathcal{T}(h)_{i+1,l} &= \mathcal{B}_{i+1,l}(S_i(h_{i,l}, 0, 0)) + \mathcal{B}_{i+1,l}(S_i(0, h_{i,r}, 0)), \quad 1 \leq i \leq N-1 \\ \mathcal{T}(h)_{i-1,r} &= \mathcal{B}_{i-1,r}(S_i(0, h_{i,r}, 0)) + \mathcal{B}_{i-1,r}(S_i(h_{i,l}, 0, 0)), \quad 2 \leq i \leq N \end{aligned} \quad (15)$$

Had we used exact absorbing boundary conditions (EABC) \mathcal{B}^{EABC} instead of the zero-th order ones (3) in equations (9)-(10), we would have with obvious abuse of notation:

$$\begin{aligned} \mathcal{B}_{i+1,l}^{EABC}(S_i^{EABC}(0, h_{i,r}, 0)) &= 0, \quad 1 \leq i \leq N-1 \\ \mathcal{B}_{i-1,r}^{EABC}(S_i^{EABC}(h_{i,l}, 0, 0)) &= 0, \quad 2 \leq i \leq N. \end{aligned} \quad (16)$$

Then, the operator would have the following form

$$\begin{aligned}\mathcal{T}^{EABC}(h)_{i+1,l} &= \mathcal{B}_{i+1,l}^{EABC}(S_i^{EABC}(h_{i,l}, 0, 0)), \quad 1 \leq i \leq N-1, \\ \mathcal{T}^{EABC}(h)_{i-1,r} &= \mathcal{B}_{i-1,r}^{EABC}(S_i^{EABC}(0, h_{i,r}, 0)), \quad 2 \leq i \leq N.\end{aligned}\quad (17)$$

The operator \mathcal{T}^{EABC} is a nilpotent operator of order $N-1$ so that the inverse of $I - \mathcal{T}^{EABC}$ is easy to compute as a finite Neumann series:

$$(I - \mathcal{T}^{EABC})^{-1} = \sum_{i=0}^{N-2} (\mathcal{T}^{EABC})^i.$$

This formula induces a convergence in $N-1$ steps of a domain decomposition method with exact absorbing boundary conditions. In practice, the absorbing boundary conditions are non exact, therefore we have

$$\begin{aligned}\mathcal{B}_{i+1,l}(S_i(0, h_{i,r}, 0)) &\neq 0, \quad 1 \leq i \leq N-1, \\ \mathcal{B}_{i-1,r}(S_i(h_{i,l}, 0, 0)) &\neq 0, \quad 2 \leq i \leq N,\end{aligned}\quad (18)$$

and we loose the nilpotency property of \mathcal{T} . This led us to define a new operator \mathcal{T}_{OSDS}

$$\begin{aligned}\mathcal{T}_{OSDS}(h)_{i+1,l} &:= \mathcal{B}_{i+1,l}(S_i(h_{i,l}, 0, 0)), \quad 1 \leq i \leq N-1 \\ \mathcal{T}_{OSDS}(h)_{i-1,r} &:= \mathcal{B}_{i-1,r}(S_i(0, h_{i,r}, 0)), \quad 2 \leq i \leq N\end{aligned}\quad (19)$$

which by definition is a nilpotent operator of order $N-1$. We propose to use this newly defined operator to build a preconditioner for (8). The left-preconditioned system reads:

$$(Id - \mathcal{T}_{OSDS})^{-1}(Id - \mathcal{T})(h) = (Id - \mathcal{T}_{OSDS})^{-1}G \quad (20)$$

More intuitively, the key idea is to cancel out the reverse contribution at the interfaces that should not happen for the exact ABC case in order to prevent spurious interface reflections from hindering the convergence. In fact, these boundary conditions at the interfaces produce spurious reflected waves that significantly increase the number of iterations to converge, in particular for heterogeneous media and high frequency regimes. Note that for a non overlapping domain decomposition, the OSDS algorithm is similar to the double sweep method of [16, 17]. Our approach addresses the case of overlapping subdomains that benefits the convergence rate.

4 Convergence rates

We first recall the convergence rates proved in [13] for the fixed point method related to the Jacobi and double sweep methods for the convection-diffusion equation and sketch how a similar estimate is derived for the OSDS algorithm. Then, we consider the Helmholtz equation.

It was proved in Theorem 2.4 of [13] that under some geometric assumptions the fixed point algorithms achieve geometric convergence with the following estimates:

Jacobi method (6):

$$\|u_i^n - u\|_{H_{st}^2(\Omega_i)} \leq C\rho^{\lfloor \frac{n}{2(N-1)} \rfloor} \sup_j \|u_j^0 - u\|_{H_{st}^2(\Omega_j)} \quad n \geq 2N+1, \quad (21)$$

Double sweep algorithm (13)-(14):

$$\|u_i^n - u\|_{H_{st}^2(\Omega_i)} \leq C\rho^n \sup_j \|u_j^0 - u\|_{H_{st}^2(\Omega_j)} \quad n \geq 3, \quad (22)$$

(writing $\lfloor . \rfloor$ for the integer part) where C and ρ are constants, $C > 0$, $0 < \rho < 1$ and $\|\cdot\|_{H_{st}^2}$ denotes some Sobolev norm.

Under the same assumptions, it can be checked that for n even, we have

$$\|u_i^n - u\|_{H_{st}^2(\Omega_i)} \leq 2\sqrt{\rho}^n \sup_j \|u_j^0 - u\|_{H_{st}^2(\Omega_j)} \quad n \geq 2, \quad (23)$$

for the fixed point method related to the overlapping splitting double sweep defined as follows:

$$(Id - \mathcal{T}_{OSDS})(h^{n+1}) = (\mathcal{T} - \mathcal{T}_{OSDS})(h^n) + G. \quad (24)$$

Note that the expression for ρ (not shown here) is the same for all these estimates. The differences lie in the exponent of ρ and in the constant. The constant C in eq. (22) may be large (see estimate (29) below) whereas in eq. (23) its value is

simply 2. A seemingly advantage of (22) with respect to (23) is the square root of ρ ratio in the convergence rate. In fact this difference is nullified when you realize that an iteration of DS takes twice as much time as an iteration of OSDS. Indeed, during one iteration the DS algorithm, only one subdomain is active at a time in the order $1 \rightarrow 2 \rightarrow \dots \rightarrow N$ and then in the reverse order $N \rightarrow N-1 \rightarrow \dots \rightarrow 1$. Whereas during one iteration of OSDS, two subdomains are active at a time in the order $1 \rightarrow 2 \rightarrow \dots \rightarrow N$ for one subdomain and concurrently in the reverse order $N \rightarrow N-1 \rightarrow \dots \rightarrow 1$ for the other one. Thus, the elapsed time of one iteration of DS is thus twice as much time as one iteration of OSDS using two cores. Note that using two cores for the DS algorithm brings no advantage in terms of elapsed time. So overall, these estimates give an edge to OSDS over DS in terms of the constants in formulas (22) and (23).

We give a few hints on the proof of (23). The convergence of OSDS depends on the spectral norm of

$$R_{OSDS} := (Id - \mathcal{T}_{OSDS})^{-1}(\mathcal{T} - \mathcal{T}_{OSDS}). \quad (25)$$

In order to estimate it, we first recall the notations and results from [13]. The operator \mathcal{T} can be written in the form of an operator valued matrix

$$\mathcal{T}(H) = \begin{bmatrix} 0 & & 0 & \times & & 0 \\ \times & \ddots & & & \ddots & \\ & \ddots & \ddots & & \ddots & \\ 0 & & \times & 0 & 0 & \times \\ \times & & 0 & 0 & \times & 0 \\ & \ddots & & & \ddots & \\ & & \ddots & & \ddots & \times \\ 0 & & & \times & 0 & 0 \end{bmatrix} \begin{bmatrix} h_{2,l} \\ \vdots \\ \vdots \\ h_{N,l} \\ h_{1,r} \\ \vdots \\ \vdots \\ h_{N-1,r} \end{bmatrix}$$

where the crosses correspond to non zero operators.

In order to write them in a compact form, we introduce four $(2N-2) \times (2N-2)$ operator valued matrices:

$$\begin{aligned} \mathcal{M}_l &= (\mathcal{M}_{l,mn})_{1 \leq m, n \leq 2N-2} \text{ with } \mathcal{M}_{l,mn} = \begin{cases} \mathcal{T}_{mn} & 1 \leq m, n \leq N-1 \\ 0 & \text{otherwise} \end{cases} \\ \mathcal{A}_l &= (\mathcal{A}_{l,mn})_{1 \leq m, n \leq 2N-2} \text{ with } \mathcal{A}_{l,mn} = \begin{cases} \mathcal{T}_{mn} & 1 \leq m \leq N-1, N \leq n \leq 2N-2 \\ 0 & \text{otherwise} \end{cases} \\ \mathcal{A}_r &= (\mathcal{A}_{r,mn})_{1 \leq m, n \leq 2N-2} \text{ with } \mathcal{A}_{r,mn} = \begin{cases} \mathcal{T}_{mn} & N \leq m \leq 2N-2, 1 \leq n \leq N-1 \\ 0 & \text{otherwise} \end{cases} \\ \mathcal{M}_r &= (\mathcal{M}_{r,mn})_{1 \leq m, n \leq 2N-2} \text{ with } \mathcal{M}_{r,mn} = \begin{cases} \mathcal{T}_{mn} & N \leq m, n \leq 2N-2 \\ 0 & \text{otherwise} \end{cases} \end{aligned}$$

so that we have $\mathcal{T} = \mathcal{M}_l + \mathcal{A}_l + \mathcal{M}_r + \mathcal{A}_r$. We recall relations (23) page 369 in [13]:

$$\begin{aligned} \mathcal{M}_r^{N-1} &= \mathcal{M}_l^{N-1} = 0; & \mathcal{M}_l \mathcal{M}_r &= \mathcal{M}_r \mathcal{M}_l = 0; & \mathcal{A}_l^2 &= \mathcal{A}_r^2 = 0 \\ \mathcal{A}_l \mathcal{M}_l &= \mathcal{A}_r \mathcal{M}_r = 0; & \mathcal{M}_l \mathcal{A}_r &= \mathcal{M}_r \mathcal{A}_l = 0 \end{aligned} \quad (26)$$

It is worth noticing that these relations come from the structure of the matrices and do not depend on the value of the coefficients.

Using these notations and the nilpotency of \mathcal{M}_l and \mathcal{M}_r , it can be checked that R_{OSDS} has the following expression:

$$R_{OSDS} = \sum_{i=0}^{N-2} \mathcal{M}_r^i \mathcal{A}_r + \sum_{i=0}^{N-2} \mathcal{M}_l^i \mathcal{A}_l.$$

Then using cancellation relations (26), it can be checked that for n even:

$$R_{OSDS}^n = \left(\sum_{i=0}^{N-2} \mathcal{M}_r^i \mathcal{A}_r \sum_{i=0}^{N-2} \mathcal{M}_l^i \mathcal{A}_l \right)^{n/2} + \left(\sum_{i=0}^{N-2} \mathcal{M}_l^i \mathcal{A}_l \sum_{i=0}^{N-2} \mathcal{M}_r^i \mathcal{A}_r \right)^{n/2}.$$

The estimate follows from the formula for ρ given in Theorem 5.1. of [13].

4.1 Application to Helmholtz equation

The above formula are obtained by algebraic means and remain thus valid if the equation to be solved is the Helmholtz equation in place of the convection-diffusion equation.

In this section, as in [13], the space \mathbb{R}^2 is decomposed into N vertical strips in the following manner: Let $\Omega_i =]l_i, L_i[\times \mathbb{R}$, $1 \leq i \leq N$ with $-\infty = l_1 < l_2 \leq L_1 < \dots < L_{i-2} < l_i \leq L_{i-1} < \dots < L_N = +\infty$, we have $\mathbb{R}^2 = \cup_{i=1}^N \Omega_i$. This simple decomposition into straight strips makes it possible to use the Fourier transform along the interfaces (the dual variable of y is denoted by ξ). It is then possible to compute the Fourier symbols of the operators of the previous section. They will be expressed in function of the symbols of the Dirichlet-to-Neumann map $\lambda(\xi)$ of a half space: for propagative modes ($|\xi| < |k|$):

$$\lambda(\xi) := Ik\sqrt{1 - \xi^2/k^2}$$

and for vanishing modes ($|\xi| > |k|$):

$$\lambda(\xi) := \sqrt{\xi^2 - k^2},$$

They will also be expressed in terms of $\rho_j(\xi)$ (the convergence rate for a decomposition of \mathbb{R}^2 into two non overlapping half spaces), an interface condition whose Fourier symbol is of the form $B := \partial_{\bar{n}} + \lambda_j(\xi)$ (in this work we have simply taken $\lambda_j(\xi) = Ik$):

$$\rho_j(\xi) := \frac{\lambda(\xi) - \lambda_j(\xi)}{\lambda(\xi) + \lambda_j(\xi)},$$

and of the width δ of the overlap between subdomains taken constant for the sake of simplicity. More specifically, we obtain the following formulas for the Fourier symbols of the different operators:

$$\begin{aligned} (A_r)_{n+N-1,n}(\xi) &= \frac{\rho_j(e^{-\lambda\delta} + e^{-\lambda(L_{n+1}-l_{n+1})})}{1 - \rho_j^2 e^{-2\lambda(L_{n+1}-l_{n+1})}}, \quad 1 \leq n \leq N-1, \\ (A_l)_{n,n+N-1}(\xi) &= \frac{\rho_j(e^{-\lambda\delta} + e^{-\lambda(L_n-l_n)})}{1 - \rho_j^2 e^{-2\lambda(L_n-l_n)}}, \quad 1 \leq n \leq N-1, \\ (M_l)_{n+1,n}(\xi) &= \frac{e^{-\lambda(L_{n+1}-l_{n+1}-\delta)}(1 - \rho_j^2)}{1 - \rho_j^2 e^{-2\lambda(L_{n+1}-l_{n+1})}}, \quad 1 \leq n \leq N-2, \\ (M_r)_{n,n+1}(\xi) &= \frac{e^{-\lambda(L_{n-N+2}-l_{n-N+2}-\delta)}(1 - \rho_j^2)}{1 - \rho_j^2 e^{-2\lambda(L_{n-N+2}-l_{n-N+2})}}, \quad N \leq n \leq 2N-3. \end{aligned} \quad (27)$$

The convergence factor ρ is given by:

$$\rho(\xi) := \|A_r(\xi)\| \|A_l(\xi)\| \left(\sum_{i=0}^{N-2} \|M_l(\xi)\|^i \right) \left(\sum_{i=0}^{N-2} \|M_r(\xi)\|^i \right),$$

and the constant C in the convergence estimates of Jacobi and DS methods, equations (21) and (22) has the following form:

$$C(\xi) := \left(1 + \frac{\rho(\xi)}{\|A_l(\xi)\|} \right) \left(1 + \frac{\rho(\xi)}{\|A_r(\xi)\|} + \frac{\rho(\xi)}{\|A_r(\xi)\| \|A_l(\xi)\|} \right).$$

These formula are identical to formula (22) of [13] except for the formula of λ and ρ_j .

We now give some estimates valid for the Helmholtz equation and our approximation $\lambda_j = Ik$ of the symbol $\lambda(\xi)$ of the Dirichlet to Neumann map. We differentiate between the propagative and vanishing modes starting with the former one. In order to simplify the expressions, we assume that all subdomains have a width at least equal to some number $H > 0$ and the overlap is smaller than $H/2$.

4.1.1 Propagative modes $|\xi| < |k|$

The expression of the two-subdomain convergence factor ρ_j is then:

$$\rho_j(\xi) = \frac{\sqrt{1 - \xi^2/k^2} - 1}{\sqrt{1 - \xi^2/k^2} + 1} \quad \text{and} \quad |\rho_j(\xi)| < 1,$$

and $\lambda(\xi)$ is a purely imaginary number so that the exponentials in formula (27) are of modulus exactly 1, so that we have the following estimates:

$$|A_r(\xi)_{n+N-1,n}|, |A_l(\xi)_{n,n+N-1}| \leq |\rho_j(\xi)| \frac{2}{1 - \rho_j^2(\xi)},$$

and

$$|(M_r(\xi))_{n,n+1}|, |(M_l(\xi))_{n+1,n}| \leq 1.$$

It is then easy to prove the following estimates:

$$\rho(\xi) \leq \rho_j(\xi)^2 \frac{4}{(1 - \rho_j^2(\xi))^2} \times (N - 1)^2, \quad (28)$$

It is interesting that in these expressions, the overlap is of no help so that convergence of the fixed point method can only be proved for small enough $|\xi/k| \leq \eta_N$ where the threshold η_N depends on the number of subdomains.

Note also that

$$C(0) \geq (N - 1)^2 \quad (29)$$

has a quadratic growth with the number of subdomains.

4.1.2 Vanishing modes $|\xi| > |k|$

The expression of the convergence factor ρ is then:

$$\rho_j(\xi) = \frac{\sqrt{\xi^2 - k^2} - Ik}{\sqrt{\xi^2 - k^2} + Ik}$$

whose modulus is exactly one and $\lambda(\xi)$ is a real positive number so that the following estimates hold:

$$|A_r(\xi)_{n+N-1,n}|, |A_l(\xi)_{n,n+N-1}| \leq 2 \frac{e^{-\lambda(\xi)\delta}}{1 - e^{-2\lambda(\xi)H}},$$

and

$$|(M_r(\xi))_{n,n+1}|, |(M_l(\xi))_{n+1,n}| \leq 2 \frac{e^{-\lambda(\xi)H/2}}{1 - e^{-2\lambda(\xi)H}}.$$

For all $\eta > 1$ and $|\xi/k| \geq \eta$, it can be proved as in [13] Lemma 6.1 that for a sufficiently large overlap δ we have

$$|\rho(\xi)| < e^{-2\delta\lambda(\xi)}. \quad (30)$$

These results show convergence for a Fourier number ξ far enough from the cut-off frequency k which makes sense since for $|\xi| = |k|$ even in the two-subdomain case the convergence factor is equal to one.

Now instead of a domain Ω equals to the plane \mathbb{R}^2 , we take an infinite waveguide $\Omega = \mathbb{R} \times (0, L)$ for some $L > 0$ with Dirichlet boundary conditions on top and bottom. Then, the above computation can be made provided that we replace the Fourier transform by Fourier series of the type

$$u(x, y) = \sum_{\xi \in \mathbb{N}^*} u_\xi \sin\left(\xi \pi \frac{y}{L}\right),$$

For that it is sufficient to substitute, in the previous formulas, ξ by $\xi\pi/L$ for $\xi \in \mathbb{N}^*$. The symbol λ of the Dirichlet to Neumann map of the half waveguide has the following expression:

$$\lambda(\xi) = \sqrt{-k^2 + (\xi\pi/L)^2}.$$

Thus if kL/π is an integer (resonant waveguide) we have $\lambda = 0$ for $\xi = kL/\pi$ whereas if kL is not an integer we never encounter the difficulty of having $\lambda = 0$.

The above estimates (28)-(30) on $\rho(\xi)$ and (29) on $C(\xi)$ apply to the estimates of convergence for the various methods (Jacobi (21), Double Sweep (22) and Overlapping Splitting Double Sweep (23)) up to a change of the H^2 norm for a norm on the Fourier transform of the unknowns for a fixed Fourier number ξ .

5 Numerical results

In this section, we present numerical results when solving the substructured equation (8) with the GMRES algorithm right preconditioned by Id (Jacobi method), $(Id - \mathcal{T}_{DS})^{-1}$ (Double sweep algorithm) and $(Id - \mathcal{T}_{OSDS})^{-1}$ (Overlapping Splitting Double sweep algorithm). The Helmholtz equation is discretized with a P1 finite element using the FreeFem++ domain specific language [11]. Note that we use a careful variational discretisation of the normal derivative ensuring that the solution obtained converges to the solution of the problem without domain decompositions.

5.1 Homogeneous waveguide

First, we consider the homogeneous waveguide test case with a layered decomposition into N subdomains. More specifically, we consider a rectangular geometry ($\Omega = [0, N] \times [0, 1]$) made of a homogeneous medium. On the upper and lower sides of the waveguide, we impose homogeneous Dirichlet conditions (cf. black lines in Figure 3). In addition, we perform a multimode excitation on the left side and we impose an absorbing boundary conditions on the right side. The global problem is written as

$$\begin{cases} (-k^2 - \Delta) u = f & \text{in } \Omega \\ (\partial_n + Ik) u = 0 & \text{on } \{x = N\} \times [0, 1] \\ (\partial_n + Ik) u = u_g & \text{on } \{x = 0\} \times [0, 1] \\ u = 0 & \text{on } [0, N] \times \{y = 0, y = 1\} \end{cases} \quad (31)$$

where $u_g = e^{-120(y-0.5)^2} \sin(\pi y)$.

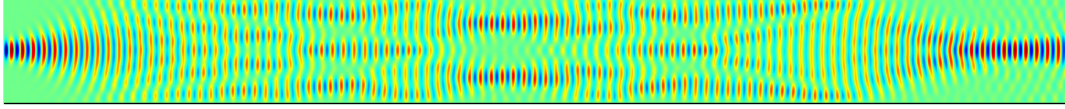


Figure 3: Homogeneous waveguide ($k = 20\pi$)

We considered two values for the wave number: $k = 20$ and $k = 20\pi$. The width of the overlap is 4 mesh size. In Tables 1 and 2 we show iteration counts. We use two stopping criteria for the residual: 10^{-6} and 10^{-3} the latter is written in brackets. As expected, the Jacobi method needs many iterations to converge. For both Jacobi and double sweep algorithms, the iteration counts vary linearly w.r.t. the number of subdomains. The iteration counts for the Overlapping Splitting Double Sweep algorithm are significantly lower and display a sublinear behavior w.r.t. the number of subdomains.

N	Jacobi	DS	OSDS
5	28 (11)	18 (7)	9 (3)
10	65 (27)	37 (15)	12 (4)
20	165 (51)	74 (36)	23 (7)
40	356 (86)	151 (72)	36 (10)
80	781 (155)	296 (144)	67 (18)

Table 1: Homogeneous waveguide, $k = 20$, $\delta = 4h$, TOL= 10^{-6} (10^{-3}), nppwl = 24, P1

N	Jacobi	DS	OSDS
5	25	16	9
10	62	33	20
20	130	76	33
40	280	170	60

Table 2: Homogeneous waveguide, $k = 20\pi$, $\delta = 4h$, TOL= 10^{-6} , nppwl = 24, P1

5.2 Influence of the overlap

We have also tested the effect of the width of the overlap on the convergence. We considered two test cases: the homogeneous waveguide (see Table 3) and the wedge (see Table 4) that is defined in more detail in § 5.4. We observe that for the waveguide solved by the Overlapping Splitting Double Sweep method, the iteration count decreases significantly with the overlap. This monotonical decrease in the iteration count contrasts with the behaviour of the other two methods. We see that for the Jacobi and double sweep (DS) methods, the overlap has a very little effect. For the Jacobi method it improves slightly the iteration counts whereas for the DS method, it might deteriorate the iteration count. For the wedge test case, all methods benefit monotonically from the size of the overlap but once again the reduction in the iteration count is more pronounced for the Overlapping Splitting Double Sweep method where the iteration count is reduced by a factor 1.83 when the overlap is increased from $2h$ to $16h$.

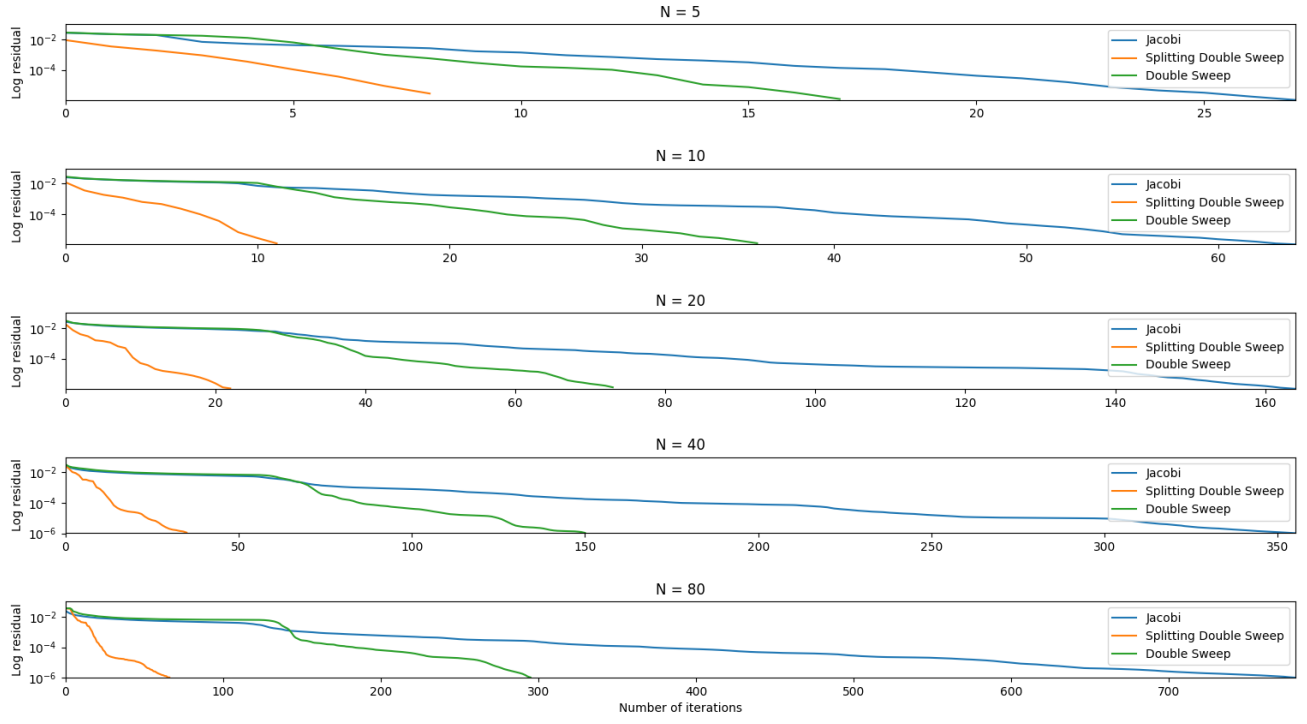


Figure 4: Homogeneous waveguide residual curves ($\text{tol} = 10^{-6}$), Jacobi in blue, DS in green and OSDS in orange

δ	Jacobi	DS	OSDS
2	159	69	27
4	165	74	23
8	160	76	20
16	143	73	18

Table 3: Homogeneous waveguide, $k = 20$, δ varies, $\text{TOL} = 10^{-6}$, $\text{nppwl} = 24$, P1

δ	Jacobi	DS	OSDS
2	259	127	97
4	245	117	83
8	221	105	69
16	202	91	53

Table 4: Wedge, $\omega = 40\pi$, δ varies, $\text{TOL} = 10^{-6}$, $\text{nppwl} = 24$, P1

5.3 Open cavity test

Same as before, the domain is rectangular with an homogeneous medium and its length increases with the number of subdomains. The open cavity test is challenging due to the homogeneous Dirichlet conditions imposed on three sides (cf. black lines in Figure 5). In addition, we perform an excitation on the left side. The Dirichlet conditions create rebounds leading to an increase in the number of reflections, this phenomenon is exacerbated for high-frequency regimes. The global problem can be written as

$$\begin{cases} (-k^2 - \Delta) u = f & \text{in } \Omega \\ (\partial_{\vec{n}} + Ik) u = g & \text{on } \Gamma \\ u = 0 & \text{on } \partial\Omega \setminus \Gamma \end{cases} \quad (32)$$

where $\Gamma := \{x = 0\} \times [0, 1]$ and $g = \exp^{-ik(x\cos(\theta) + y\sin(\theta))}$, $\theta = \frac{\pi}{8}$. It corresponds to an incident plane wave propagating at an angle $\frac{\pi}{8}$ w.r.t. to the horizontal direction, see Fig. 5. This creates numerous reflections on the lateral boundaries of the open cavity.

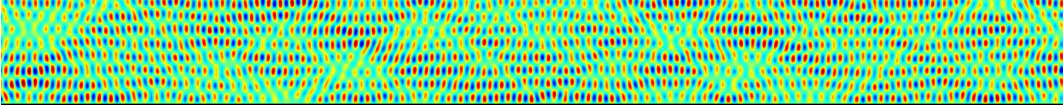


Figure 5: Open cavity solution ($k = 20\pi$)

Iteration counts are given in Tables 5 and 6 for two wave numbers. One can notice that we took an overlap of $8h$ instead of $4h$ for the waveguide because we want to take advantage of the fact that the overlap contributes to accelerate convergence. Once again, for a given number of subdomains, the Overlapping Splitting DS method is systematically better than the other methods. As for the scalability, we observe that in terms of the number of subdomains, the iteration count varies surlinearly for the Jacobi method, linearly for the DS method and sublinearly for the Overlapping Splitting DS method.

N	Jacobi	DS	OSDS
5	54	29	15
10	124	56	19
20	279	109	29
40	551	202	45
80	+1200	416	78

Table 5: Open cavity, $k = 20$, $\delta = 8h$, $\text{TOL}=10^{-6}$, $nppwl = 24$, P1

N	Jacobi	DS	OSDS
5	72	47	31
10	154	94	47
20	331	223	82
40	754	453	149

Table 6: Open cavity, $k = 20\pi$, $\delta = 8h$, $\text{TOL}=10^{-6}$, $nppwl = 24$, P1

5.4 Wedge test

We consider the classical test case of the wedge, see e.g. [16], a rectangular domain $[0, 600] \times [0, 1000]$ with three different velocities in regions separated by non-parallel boundaries (Fig. 7 left). Starting from the top, the velocities are $c = 2000$, $c = 1500$ and $c = 3000$. Sommerfeld conditions are imposed on the bottom, right and left boundaries. The abrupt variations of the wavenumber produce internal reflections in different directions. A typical solution is shown on Figure 7 right. The global problem can be written as

$$\begin{cases} (-k(x, y)^2 - \Delta) u = f & \text{in } \Omega \\ (\partial_{\vec{n}} + Ik) u = g & \text{on } \Gamma_R \\ (\partial_{\vec{n}} + Ik) u = 0 & \text{on } \partial\Omega \setminus \Gamma_R \end{cases} \quad (33)$$

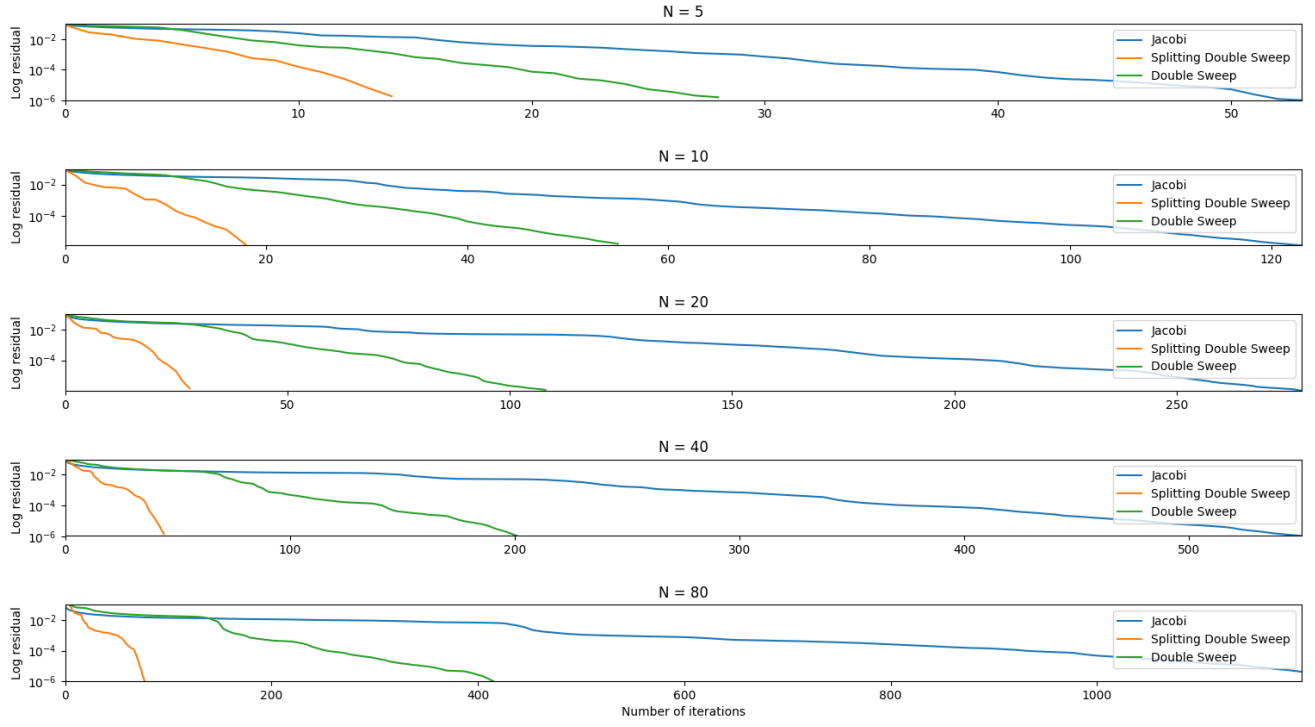


Figure 6: Open cavity residual curves ($\text{tol} = 10^{-6}$), Jacobi in blue, DS in green and OSDS in orange

where $\Gamma_R := [0, 600] \times \{y = 1000\}$ and $g = e^{-120(y-0.5)^2} \sin(\pi y)$.

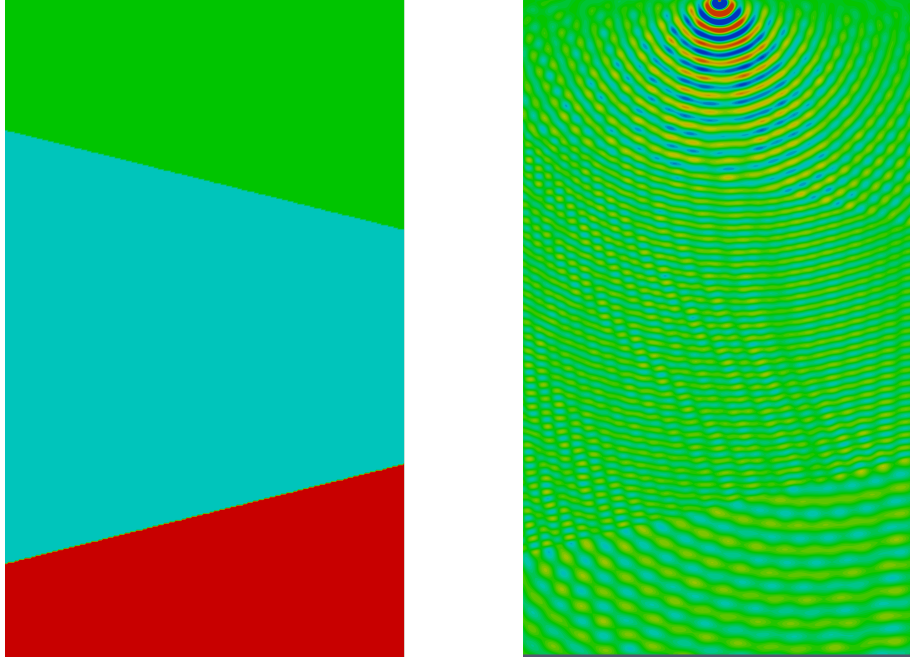


Figure 7: Heterogeneous media: Wedge (**Left**: Velocity model, **Right**: Solution (real) for $\omega = 160\pi$)

Convergence curves are plotted in Fig. 8 and iteration counts are given in Tables 7 and 8. The OSDS method is clearly superior to the Jacobi and DS methods. When increasing the number of subdomains, the ratio in favor of the OSDS method compared to the DS method increases up to reaching a value of nearly 4 for a domain decomposition into 40 strips. Interestingly, we see that for a low tolerance on the residual ($\text{TOL} = 10^{-3}$), the OSDS iteration counts are almost independent of the number of subdomains. Note also that compared to the DS method, the convergence curves of the OSDS method does not suffer of any stagnation.

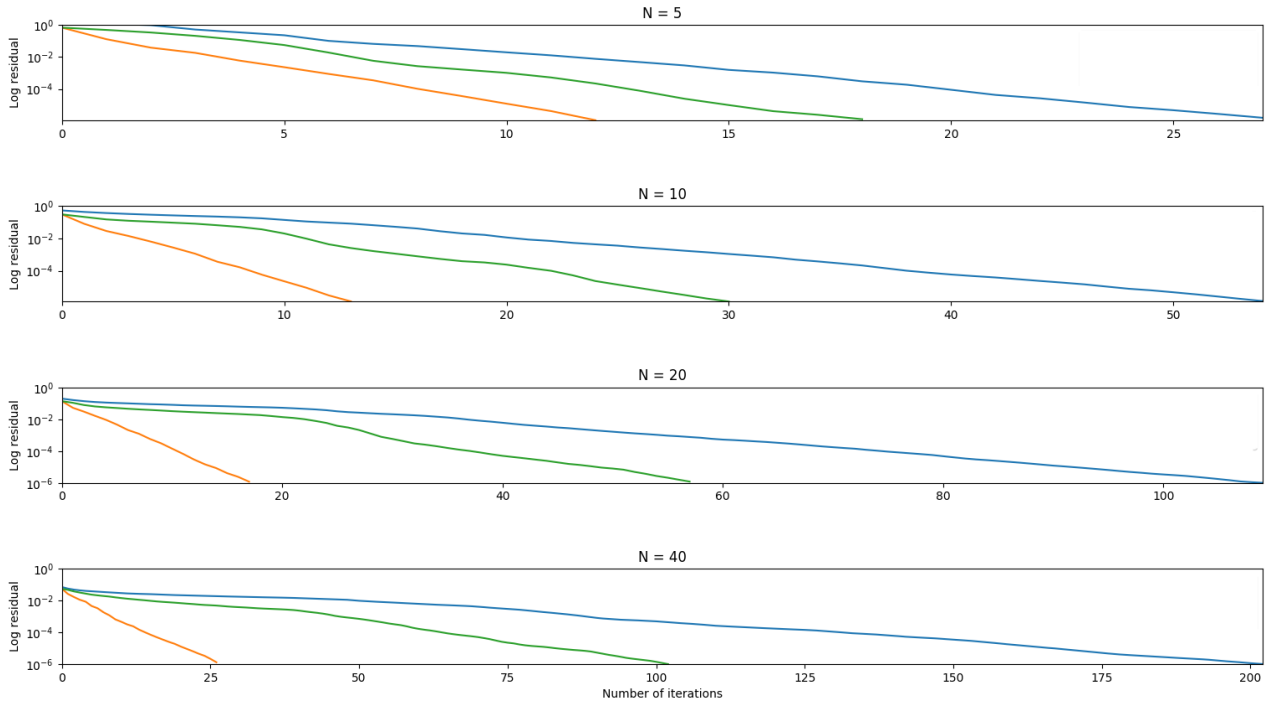


Figure 8: Wedge residual curves ($\text{tol} = 10^{-6}$), Jacobi in blue, DS in green and OSDS in orange

N	Jacobi	DS	OSDS
5	28 (17)	19 (11)	13 (6)
10	55 (31)	31 (16)	14 (7)
20	110 (55)	58 (29)	18 (8)
40	203 (88)	103 (47)	27 (9)

Table 7: Wedge, $\omega = 40\pi$, $\delta = 16h$, $\text{TOL}=10^{-6}(10^{-3})$, $nppwl = 24$, P1

N	Jacobi	DS	OSDS
5	28 (15)	18 (10)	12 (5)
10	56 (30)	31 (15)	14 (6)
20	111 (53)	57 (28)	18 (7)
40	206 (85)	111 (55)	30 (9)

Table 8: Wedge, $\omega = 60\pi$, $\delta = 16h$, $\text{TOL}=10^{-6}(10^{-3})$, $nppwl = 24$, P1

6 Prospects

We have introduced an overlapping splitting double sweep algorithm which yields improved convergence for various problems: the waveguide, the open cavity and wedge test cases. It is analyzed for a plane decomposed into vertical strips. Many aspects deserve further investigations, in this section we only list some of them. As previously mentioned, for a first study of the new algorithm we only use first-order absorbing boundary conditions at the interfaces. It is known that higher-order ABC lead to drastically better stability properties and to a quicker convergence. This should reflect in better iteration counts for all methods. Also, an intrinsic problem with both double sweep and overlapping splitting double sweep methods is that due to the sequentiality of the algorithm, subdomains are idle most of the time. To be more precise, in a double sweep, only one process is active at a time whereas in an overlapping splitting double sweep, two processes are active at a time (one for the left sweep and one for the right sweep performed concurrently). A solution to overcome this is to introduce a

pipelining technique that can be applied to multiple right-hand sides problems to improve parallelism and achieve significant speed-ups, see [17]. As a last remark, note that in a volumic version of the algorithm the local solve induced by the definition of the overlapping splitting double sweep operator \mathcal{T}_{OSDS} , eq. (19) could be replaced by a cheaper approximate solve such as incomplete factorizations [8].

References

- [1] Xavier Antoine, Yassine Boubendir, and Christophe Geuzaine. A quasi-optimal non-overlapping domain decomposition algorithm for the Helmholtz equation. *Journal of Computational Physics*, 231(2):262–280, 2012.
- [2] Christiaan C. Stolk. A rapidly converging domain decomposition method for the Helmholtz equation. *Journal of Computational Physics*, 241:240–252, May 2013.
- [3] Zhiming Chen and Xueshuang Xiang. A source transfer domain decomposition method for helmholtz equations in unbounded domain. *SIAM Journal on Numerical Analysis*, 51(4):2331–2356, 2013.
- [4] Bruno Després. Domain decomposition method and the helmholtz problem. In *Mathematical and numerical aspects of wave propagation phenomena (Strasbourg, 1991)*, pages 44–52, Philadelphia, PA, 1991. SIAM.
- [5] Bruno Després, Patrick Joly, and Jean E. Roberts. A domain decomposition method for the harmonic Maxwell equations. In *Iterative methods in linear algebra (Brussels, 1991)*, pages 475–484, Amsterdam, 1992. North-Holland.
- [6] Victorita Dolean, Pierre Jolivet, and Frédéric Nataf. *An Introduction to Domain Decomposition Methods: algorithms, theory and parallel implementation*. SIAM, 2015.
- [7] Björn Engquist and Lexing Ying. Sweeping preconditioner for the Helmholtz equation: Hierarchical matrix representation. *Communications on Pure and Applied Mathematics*, 64(5):697–735, 2011. [_eprint: https://onlinelibrary.wiley.com/doi/pdf/10.1002/cpa.20358](https://onlinelibrary.wiley.com/doi/pdf/10.1002/cpa.20358).
- [8] Björn Engquist and Lexing Ying. Sweeping Preconditioner for the Helmholtz Equation: Moving Perfectly Matched Layers. *Multiscale Modeling & Simulation*, 9(2):686–710, April 2011. Publisher: Society for Industrial and Applied Mathematics.
- [9] Martin J. Gander, Frédéric Magoulès, and Frédéric Nataf. Optimized Schwarz methods without overlap for the Helmholtz equation. *SIAM J. Sci. Comput.*, 24(1):38–60, 2002.
- [10] Martin J Gander and Hui Zhang. A class of iterative solvers for the helmholtz equation: Factorizations, sweeping preconditioners, source transfer, single layer potentials, polarized traces, and optimized schwarz methods. *Siam Review*, 61(1):3–76, 2019.
- [11] F. Hecht. New development in Freefem++. *J. Numer. Math.*, 20(3-4):251–265, 2012.
- [12] Pierre-Louis Lions. On the Schwarz alternating method. III: a variant for nonoverlapping subdomains. In Tony F. Chan, Roland Glowinski, Jacques Périaux, and Olof Widlund, editors, *First International Symposium on Domain Decomposition Methods for Partial Differential Equations*, Philadelphia, PA, 1990. SIAM.
- [13] Frédéric Nataf and Francis Nier. Convergence rate of some domain decomposition methods for overlapping and nonoverlapping subdomains. *Numerische Mathematik*, 75(3):357–77, 1997.
- [14] Frédéric Nataf, Francois Rogier, and Eric de Sturler. Optimal interface conditions for domain decomposition methods. Technical Report 301, CMAP (Ecole Polytechnique), 1994.
- [15] H. A. Schwarz. Über einen Grenzübergang durch alternierendes Verfahren. *Vierteljahrsschrift der Naturforschenden Gesellschaft in Zürich*, 15:272–286, 1870.
- [16] A. Vion and C. Geuzaine. Double sweep preconditioner for optimized Schwarz methods applied to the Helmholtz problem. *Journal of Computational Physics*, 266:171–190, June 2014.
- [17] A. Vion and C. Geuzaine. Parallel Double Sweep Preconditioner for the Optimized Schwarz Algorithm Applied to High Frequency Helmholtz and Maxwell Equations. In Thomas Dickopf, Martin J. Gander, Laurence Halpern, Rolf Krause, and Luca F. Pavarino, editors, *Domain Decomposition Methods in Science and Engineering XXII*, Lecture Notes in Computational Science and Engineering, pages 239–247, Cham, 2016. Springer International Publishing.
- [18] Leonardo Zepeda-Núñez and Laurent Demanet. The method of polarized traces for the 2D Helmholtz equation. *Journal of Computational Physics*, 308:347–388, March 2016.